

See discussions, stats, and author profiles for this publication at: <https://www.researchgate.net/publication/231396214>

# Asymmetrical Concentration Fluctuations in the Autocatalytic Bromate–Bromide Catalyst Reaction and in the Oscillatory Belousov–Zhabotinsky Reaction in Closed Reactor: Stirring Effe...

ARTICLE in THE JOURNAL OF PHYSICAL CHEMISTRY · NOVEMBER 1995

Impact Factor: 2.78 · DOI: 10.1021/j100048a011

---

CITATIONS

23

---

READS

28

2 AUTHORS, INCLUDING:



Vladimir K Vanag

Immanuel Kant Baltic Federal University

78 PUBLICATIONS 2,126 CITATIONS

SEE PROFILE

## Asymmetrical Concentration Fluctuations in the Autocatalytic Bromate-Bromide Catalyst Reaction and in the Oscillatory Belousov-Zhabotinsky Reaction in Closed Reactor: Stirring Effects

Vladimir K. Vanag, and Dmitrii P. Melikhov

*J. Phys. Chem.*, **1995**, 99 (48), 17372-17379 • DOI: 10.1021/j100048a011

Downloaded from <http://pubs.acs.org> on January 14, 2009

### More About This Article

---

The permalink <http://dx.doi.org/10.1021/j100048a011> provides access to:

- Links to articles and content related to this article
- Copyright permission to reproduce figures and/or text from this article



**ACS Publications**  
High quality. High impact.

The Journal of Physical Chemistry is published by the American Chemical Society,  
1155 Sixteenth Street N.W., Washington, DC 20036

# Asymmetrical Concentration Fluctuations in the Autocatalytic Bromate–Bromide–Catalyst Reaction and in the Oscillatory Belousov–Zhabotinsky Reaction in Closed Reactor: Stirring Effects

Vladimir K. Vanag\* and Dmitrii P. Melikhov

Department of Photochemistry, N. N. Semenov Institute of Chemical Physics, Russian Academy of Sciences, 117421, Novatorov Str., 7A, Moscow, Russia

Received: June 2, 1995; In Final Form: September 5, 1995<sup>⊗</sup>

The effect of stirring on the autocatalytic bromate–bromide–catalyst reaction has been studied at various initial concentrations of bromate,  $[\text{BrO}_3^-]_0$ , bromide,  $[\text{Br}^-]_0$ , and catalyst,  $[\text{C}]_0$ , in a batch closed reactor. As catalysts, ferroin and  $\text{Ce}^{\text{III}}$  were used. An enhancement of the stirring rate was found to lead to a longer induction period  $T_{\text{ind}}$  of the autocatalytic reaction. A hypothesis has been substantiated that the magnitude of the stirring effect, expressed as  $T_{\text{ind}}^{\text{max}}/T_{\text{ind}}^{\text{min}}$ , is determined by the rate of  $[\text{Br}^-]$  approaching the critical concentration  $[\text{Br}^-]_{\text{cr}}$  and by the amplitude of asymmetrical nonequilibrium fluctuations. When this rate decreases in response to larger  $[\text{Br}^-]_0$  or smaller  $[\text{BrO}_3^-]_0$ , as well as when the fluctuation amplitude grows in response to larger  $[\text{C}]_0$ , the magnitude of  $T_{\text{ind}}^{\text{max}}/T_{\text{ind}}^{\text{min}}$  increases. The role of nuclei has been discussed. The stirring effect in the oscillatory Belousov–Zhabotinsky reaction and in the autocatalytic bromate–bromide–catalyst reaction was shown to have the same origin.

## 1. Introduction

Many theoretical<sup>1–13</sup> and experimental<sup>14–26</sup> studies have been accumulated to date on the stirring effects in oscillatory chemical reactions. These effects manifest themselves as changes in the oscillatory period and amplitude<sup>15,16</sup> and even as the secession<sup>25</sup> or reappearance<sup>4</sup> of oscillations. The authors explain these effects by various means: by variation in the rates with which volatile intermediates, such as oxygen<sup>15a,16a,17</sup> and bromine,<sup>21, 25b</sup> are transferred between the reaction mixture and atmosphere; by the absorption of intermediates, i.e., bromine, onto the hydrophobic walls of the reactor, Pt-electrode, or stirrer;<sup>23</sup> in the case of a continuously stirred tank reactor (CSTR), by the macroheterogeneities appearing with incomplete mixing of the feed streams.<sup>12,13,16b,24,26</sup>

However, not all the stirring effects observed may be explained by these rather plain reasons. Some authors suggest that the stirring effect may be caused by the concentration fluctuations resulting from the interaction between fast chemical reactions and turbulent transport of substances.<sup>11,16c,d,18–21,25a</sup> These concentration fluctuations were recorded by Menzinger et al.<sup>16a,c</sup> with the aid of the Pt-microelectrodes. One of the most vivid manifestation of the stirring effect is an increase in the induction period  $T_{\text{ind}}$  of the autocatalytic reactions with more intensive stirring. This is observed for the Briggs–Rauscher (BR) reaction,<sup>21a</sup> the chlorite–iodide reaction,<sup>20a</sup> and the chlorite–thiosulfate reaction.<sup>20b</sup> A similar phenomenon is also observed for the Belousov–Zhabotinsky (BZ) reaction, where a growth in stirring intensity leads to an increase in the oscillation period.<sup>15a,16,19,22</sup>

Earlier,<sup>21a,b</sup> we have discovered the effect of stirring on the induction period  $T_{\text{ind}}$  of the autocatalytic reaction of iodide and iodine production in the BR reaction under batch conditions. As the stirring rate grows, the period  $T_{\text{ind}}$  increases in a S-like manner. Special experiments showed<sup>21c,d</sup> that the stirring effect is not concerned with iodine sorption on solid surfaces, with macroheterogeneities that are likely to occur as a result of nonuniform irradiation of the reactor, and with an oxygen and

iodine exchange with the atmosphere. Having excluded all these possibilities, we proved by contradiction that the stirring effect is connected with the effects of fluctuations or nuclei on the dynamics of the averages.<sup>21a,b</sup> By nuclei, we mean short-living, accidentally appearing microvolumes (MVs), where autocatalysis induced by the large-scale fluctuations starts much earlier than in the rest of the reactionary volume.

The idea of nuclei formation has been proposed long ago by Nicolis et al.<sup>1,27</sup> and Boissonade et al.,<sup>2,28</sup> although after the publication of Horsthemke and Hannon,<sup>3</sup> the number of the proponents of this theory decreased. Recently, however, this idea has been used again for the explanation of the stirring effect in the BZ<sup>4</sup> and BR<sup>21a,b</sup> reactions.

**Hypothesis.** From our point of view, the idea of nuclei formation can be applied to the explanation of stirring effects as follows. It is a well-known fact that without stirring the diffusion-controlled reaction between reagents A and B forms microheterogeneous areas, where this or that participant of the reaction prevails (clusterization effect).<sup>29</sup> Stirring, however, always smoothes out the spatial nonequilibrium fluctuations of reagent concentrations. With infinitely vigorous stirring, the liquid is characterized by a well-developed homogeneous turbulence, and the distribution of concentration fluctuations in the liquid elements of any size follows the Poisson equation.<sup>5,21b,30</sup>

Nonlinear chemical reactions coupled with diffusion-controlled reactions may enhance nonequilibrium fluctuations in the concentrations of reagents A and B,<sup>6,7</sup> thus prohibiting stirring of a relatively low intensity from homogenizing the system. This phenomenon should reach prominence in nonequilibrium systems with critical or bifurcation points, e.g., in oscillatory chemical reactions.<sup>2b</sup> If the critical concentration of any intermediate, for instance, B, is achieved in several MVs owing to anomalous nonequilibrium fluctuations,  $\delta[\text{B}]_{\text{ne}}$ , then the stirring rate, which affects the fluctuation amplitude  $\langle(\delta[\text{B}]_{\text{ne}})^2\rangle^{1/2}$ , the lifetime of the fluctuations, the spatial and time correlation functions may markedly affect system dynamics as a whole and even change the reaction mode. Here,  $\delta[\text{B}]_{\text{ne}} = \langle[\text{B}]_i\rangle - [\text{B}]_i(\mathbf{r}, t)$ , where  $[\text{B}]_i(\mathbf{r}, t)$  is the local concentration

<sup>⊗</sup> Abstract published in *Advance ACS Abstracts*, October 15, 1995.

in the MV with the radius vector  $r$  of this MV center at the moment  $t$  and  $\langle \dots \rangle$  denotes the ensemble average.

In order that the effect of nonequilibrium fluctuations and, hence, of the stirring rate on the dynamics of the averages observed be prominent, it is necessary, *first*, that the system, obeying ordinary differential equations for the averages (i.e., without regard for fluctuations), remains near the critical point,  $[B]_{cr}$ , long enough. This requirement entails another one for the nonequilibrium evolutionary system of its low rate of approach to the critical point.

The analogous idea about the probability of finding the system in one of the many finite states after its passing through the bifurcation point was suggested by Kondepudi,<sup>31</sup> and Zeldovich with Mikhailov,<sup>32</sup> who studied the process of symmetry breaking in the initially symmetrical systems. They showed that an asymmetric effect on the system (bias), although small in comparison to the fluctuation amplitude, may notably affect the probability of the system achieving this or that state only on condition that its passage through the bifurcation point is slow. In the case of the simple autocatalytic reactions described by the following equations<sup>21b</sup>

$$d[A]/dt = \gamma[A] - k_{AB}[A][B] - \beta[A]^2 \quad (1)$$

$$d[B]/dt = -k_{AB}[A][B] \quad (2)$$

the finite state of the system is defined uniquely. Nevertheless, from our point of view, fluctuations here may affect the dynamics of the averages but only in the case where a system passes through the critical point,  $[B]_{cr} = \gamma/k_{AB}$ , slowly. More detailed information about systems 1 and 2 and their behavior near the critical point is in the Supporting Information.

Because the concentration of  $B_i$  fluctuates, the duration of the system's stay near the critical point depends on how long the critical concentration is in the range of the nonequilibrium fluctuations of  $[B]$ ,  $\langle [B]_i \rangle$ ,  $\langle [B]_i \rangle - \langle \delta[B]_{ne} \rangle^{2/3}$ . The larger the amplitude of nonequilibrium fluctuations,  $\langle \delta[B]_{ne} \rangle^{2/3}$ , and the smaller the rate of the system approach to the critical point, the longer the system's stay near the critical point and the larger the effect that the fluctuations, lowering  $[B]$  to  $[B] < [B]_{cr}$ , manage to produce on the evolution of the averages before the system reaches  $[B]_{cr}$ . As the stirring rate decreases, the value of  $\delta[B]_{ne}$  increases. Thus, the *second requirement* for stirring to affect the system dynamics is a rather high amplitude of nonequilibrium fluctuations.

It is a well-known fact that the fluctuation amplitude depends on the linear size of a given MV. The smaller the volume, the smaller the number of molecules in it and the higher the relative amplitude  $\langle \delta[B]_p \delta[B]_p \rangle^{1/2} / \langle [B] \rangle$  of equilibrium Poissonian fluctuations. We are interested, however, in nonequilibrium fluctuations which have their own scale of coherence<sup>27,33</sup> being approximately equal to the correlation length,  $l_{corr}$ . Therefore, we should consider MV with the size on the order of  $l_{corr}$  when determining fluctuation amplitude. The correlation length of nonequilibrium fluctuations depends on the reagent concentrations, reaction rate constants, and the diffusion coefficient.<sup>33</sup> For the bimolecular reaction between molecules A and B, proceeding with the rate constant  $k_{AB}$  and under the condition of autocatalytic production of reagent A with constant  $\gamma$  ( $s^{-1}$ ) (see eqs 1 and 2), the length  $l_{corr}$  is determined<sup>21b</sup> as

$$l_{corr} = (2D/(k_{AB}([A] + [B]) - \gamma))^{1/2} \quad (3)$$

where  $D = D_o + D_{turb}$ ,  $D_o$  is the molecular diffusion coefficient, and  $D_{turb}$  is the turbulent diffusion coefficient. The assessments show<sup>21b</sup> that  $l_{corr}$  is between 10 and 100  $\mu m$ , and the amplitude

of nonequilibrium fluctuations may be tens or hundreds of a percent larger than the amplitude of Poissonian fluctuations. The smaller the  $D$ , the larger the fluctuation amplitude. To our regret, we do not know of any experimental or theoretical study performed thus far where the extent and the manner of the enhancement of Poissonian fluctuations have been shown for nonlinear nonequilibrium systems.

Finally, on the basis of the notion of the correlation length of nonequilibrium fluctuations, we can specify the *third requirement* for the stirring effect to occur. Stirring may notably affect the amplitude of nonequilibrium fluctuations, and, hence, the system dynamics, if the correlation length  $l_{corr}$  of the concentration fluctuations of the reaction key intermediate coincides or is compatible with the inner scale of turbulence  $L_k$ ,<sup>21b,16</sup> where  $L_k$  is the Kolmogorov length.<sup>34</sup> The Kolmogorov length specifies the scale in which the energy of fluid turbulence dissipates as heat owing to friction forces while stochastic pulsations in the rate of fluid elements turn into laminar motion. For the stirrers most commonly used in laboratory practice, with  $d \approx 1$  cm and rotational speed  $u = 100-1000$  rpm,  $L_k$  varies from 60  $\mu m$  to 10–8  $\mu m$ , i.e., in the same range as  $l_{corr}$ . As the stirring rate grows,  $L_k$  decreases as  $u^{-3/4}$  and turbulent pulsations penetrate deeper, breaking concentration correlations and decreasing the amplitude of nonequilibrium fluctuations, as well as the lifetime of spatial microheterogeneities. If the correlation lengths are small,  $\approx 10$   $\mu m$ , the stirring effect may be observed only at high stirring rates.

Thus, it follows from our hypothesis that along with the presence of fast (close to diffusion-controlled) reactions, the determining values for the stirring effect are (i) the rate of a system approach to the critical point, (ii) the amplitude of nonequilibrium fluctuations, and (iii) the correlation length of fluctuations, which should be compatible with the Kolmogorov length.

The goal of our work is to test this hypothesis. For this purpose we chose the autocatalytic reaction of ferroin and/or cerium(III) oxidation by bromate with initial additions of bromide. This reaction is a constituent of a well-known BZ reaction, whose rate constants are all known. If our hypothesis were true, we should not only discover the stirring effect in this reaction, but also be able to control, in terms of our theory, the magnitude of the effect by consequently changing the initial concentrations of the reagents.

## 2. Theoretical Predictions

Before proceeding to the experiment, we consider how we can affect the rate of the system approach to the critical concentration, the amplitude of nonequilibrium fluctuations, and the correlation length.

**Variation in Bromide Concentration.** First, we show that the initial concentration of bromide,  $[Br^-]_o$ , efficiently controls the rate of approach of the current bromide concentration,  $[Br^-]$ , to the critical concentration,  $[Br^-]_{cr}$ . To this end let us use the Noyes–Field–Thompson (NFT) mechanism<sup>35</sup> with coefficients in this model as updated by Field and Försterling (FF).<sup>36</sup> Tables 1 and 2 present the reactions and their rate constants used for the simulation of cerium and ferroin systems.

From schemes R1–R6, the critical concentration of bromide,  $[Br^-]_{cr}$ , is determined from the equality of the rates of forward reactions R2 and R5 and equals  $k_5[BrO_3^-]/k_2 = 1.4 \times 10^{-5}$   $[BrO_3^-]$ . After  $[Br^-]$  is lowered below the critical concentration, an autocatalytic growth of  $[HBrO_2]$  (reactions R5 + 2(R6)) starts, accompanied by the exponential growth in the concentration of the oxidized form of a catalyst,  $Ce^{IV}$  in a given case. Figure 1 shows the typical kinetic curves for the reactionary

TABLE 1: NFT Reactions and their FF Rate Constants

$\text{H}^+ + \text{Br}^- + \text{HOBr} \leftrightarrow \text{Br}_2 + \text{H}_2\text{O}$	(R1)	$k_1 = 8 \times 10^9 \text{ M}^{-2} \text{ s}^{-1}$	$k_{-1} = 110 \text{ s}^{-1}$
$\text{H}^+ + \text{Br}^- + \text{HBrO}_2 \leftrightarrow 2\text{HOBr}$	(R2)	$k_2 = 3 \times 10^6 \text{ M}^{-2} \text{ s}^{-1}$	$k_{-2} = 2 \times 10^{-5} \text{ M}^{-1} \text{ s}^{-1}$
$2\text{H}^+ + \text{Br}^- + \text{BrO}_3^- \leftrightarrow \text{HBrO}_2 + \text{HOBr}$	(R3)	$k_3 = 2 \text{ M}^{-2} \text{ s}^{-1}$	$k_{-3} = 3.2 \text{ M}^{-1} \text{ s}^{-1}$
$2\text{HBrO}_2 \leftrightarrow \text{HOBr} + \text{BrO}_3^- + \text{H}^+$	(R4)	$k_4 = 3 \times 10^3 \text{ M}^{-1} \text{ s}^{-1}$	$k_{-4} = 10^{-8} \text{ M}^{-2} \text{ s}^{-1}$
$\text{H}^+ + \text{BrO}_3^- + \text{HBrO}_2 \leftrightarrow 2\text{BrO}_2^* + \text{H}_2\text{O}$	(R5)	$k_5 = 42 \text{ M}^{-2} \text{ s}^{-1}$	$k_{-5} = 4.2 \times 10^7 \text{ M}^{-1} \text{ s}^{-1}$
$\text{H}^+ + \text{BrO}_2^* + \text{Ce}^{\text{III}} \leftrightarrow \text{HBrO}_2 + \text{Ce}^{\text{IV}}$	(R6)	$k_6 = 8 \times 10^4 \text{ M}^{-2} \text{ s}^{-1}$	$k_{-6} = 8.9 \times 10^3 \text{ M}^{-1} \text{ s}^{-1}$

TABLE 2: Additional Reactions to the R1–R5 Reactions Presented in Table 1 with Ferriin as a Catalyst

$\text{H}^+ + \text{BrO}_2^* + \text{ferriin} \leftrightarrow \text{HBrO}_2 + \text{ferriin}$	(R6)	$k_6 = 10^8 \text{ M}^{-2} \text{ s}^{-1}$ <sup>43</sup>	$k_{-6} = 3.3 \text{ M}^{-1} \text{ s}^{-1}$
$2 \text{ ferriin} + \text{Br}_2 \rightarrow 2 \text{ ferriin} + 2\text{Br}^-$	(R7)	$k_7 = 2 \text{ M}^{-1} \text{ s}^{-1}$ <sup>39</sup>	$k_{-7} = 0$

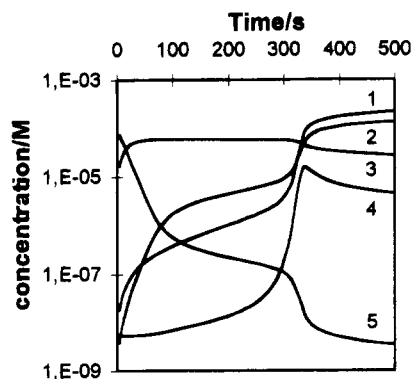


Figure 1. Kinetic curves of intermediate concentrations in the bromate-bromide- $\text{Ce}^{\text{III}}$  system: (1),  $[\text{Ce}^{\text{IV}}]$ ; (2),  $[\text{HOBr}]$ ; (3),  $[\text{Br}_2]$ ; (4),  $[\text{HBrO}_2]$ ; (5),  $[\text{Br}^-]$ . Initial conditions are  $[\text{Ce}^{\text{III}}]_0 = 10^{-3} \text{ M}$ ,  $[\text{Br}^-]_0 = 10^{-4} \text{ M}$ ,  $[\text{BrO}_3^-]_0 = 0.01 \text{ M}$ ,  $[\text{H}^+]_0 = 0.8 \text{ M}$ , and  $[\text{Ce}^{\text{IV}}]_0 = [\text{HOBr}]_0 = [\text{Br}_2]_0 = [\text{HBrO}_2]_0 = 0$ .

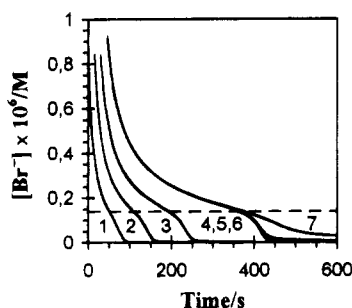


Figure 2. Variation of  $[\text{Br}^-]$  vs time in the bromate-bromide- $\text{Ce}^{\text{III}}$  system calculated on the basis of reactions R1–R6 at various initial concentrations of bromide and cerium ions. Initial concentrations are the following:  $[\text{BrO}_3^-]_0 = 0.01 \text{ M}$ ;  $[\text{H}^+]_0 = 0.8 \text{ M}$ ; (1)–(4),  $[\text{Ce}^{\text{III}}]_0 = 1.28 \times 10^{-3} \text{ M}$ ; (1)  $[\text{Br}^-]_0 = 1.73 \times 10^{-5} \text{ M}$ , (2),  $[\text{Br}^-]_0 = 4.33 \times 10^{-5} \text{ M}$ ; (3),  $[\text{Br}^-]_0 = 8.65 \times 10^{-5} \text{ M}$ ; (4)–(7),  $[\text{Br}^-]_0 = 1.73 \times 10^{-4} \text{ M}$ ; (5)  $[\text{Ce}^{\text{III}}]_0 = 10^{-2} \text{ M}$ ; (6)  $[\text{Ce}^{\text{III}}]_0 = 5 \times 10^{-4} \text{ M}$ ; (7)  $[\text{Ce}^{\text{III}}]_0 = 10^{-4} \text{ M}$ . Dashed line is the critical concentration of bromide ions,  $[\text{Br}^-]_{\text{cr}} = (k_5/k_2)[\text{BrO}_3^-]_0 = 0.14 \times 10^{-6} \text{ M}$ .

intermediates obtained as a result of a computer simulation of equations R1–R6 by the Gear method.<sup>37</sup> As is seen in Figure 1, for about 50 s after the reagents mixing,  $[\text{Br}_2]$  and  $[\text{HOBr}]$  are rapidly increasing at the expense of  $[\text{Br}^-]$ , and then a smooth fall of  $[\text{Br}_2]$  and  $[\text{Br}^-]$  follows. After about 300 s from the start of the reaction,  $[\text{Br}^-]$  reaches the critical concentration,  $[\text{Br}^-]_{\text{cr}}$ , and an autocatalytic reaction of  $[\text{HBrO}_2]$  production starts, accompanied by the exponential growth of  $[\text{Ce}^{\text{IV}}]$  and  $[\text{HOBr}]$ . The results of computation of the  $[\text{Br}^-]$  changes vs time at various initial bromide concentrations,  $[\text{Br}^-]_0$ , are shown in Figure 2. As is seen in Figure 2, the larger the initial concentration of bromide ions, the smaller the rate with which its current concentration approaches the critical value  $[\text{Br}^-]_{\text{cr}}$ .

In the case of using ferriin as a catalyst, schemes R1–R6 do not take into account all the important reactions, which entails a notable discrepancy between theoretically predicted and experimentally obtained curves. To eliminate this drawback, a

number of authors consider additional reactions between ferriin and bromine derivatives.<sup>38,39a</sup> We also took into account the most important, to our mind, reaction between ferriin and bromine,<sup>39b</sup> thus providing a good correspondence between the observed and computed curves. Thus, when simulating the ferriin system, we used reactions R1–R5 from Table 1 and reactions R6–R7 from Table 2. The calculations showed (not presented; see Supporting Information) that the rate of  $[\text{Br}^-]$  approaching the critical concentration in the ferriin system decreases with  $[\text{Br}^-]_0$  growth, the curves being of the same type as those in Figure 2. Thus, according to our hypothesis, the magnitude of the stirring effect should increase with the  $[\text{Br}^-]_0$  growth.

**Variation in Catalyst Concentration.** Let us show now that in order to control the amplitude of nonequilibrium fluctuations, we may change the catalyst concentration. In fact, if autocatalysis starts in some microvolume as large as  $l_{\text{corr}}$ , where the inequality  $[\text{Br}^-] < [\text{Br}^-]_{\text{cr}}$  holds (let us name this microvolume a nucleus),  $\text{BrO}_2^*$  radicals are produced there in the course of reaction R5. A characteristic time for  $\text{BrO}_2^*$  turning into  $\text{HBrO}_2$  in reaction R6 is determined by  $(k_6[\text{H}^+][\text{red}])^{-1}$ , where  $[\text{red}]$  is the concentration of the reduced form of a catalyst. A characteristic time for  $\text{BrO}_2^*$  radical diffusing for a length of  $l_{\text{corr}}$  equals  $l_{\text{corr}}^2/D$ . If the inequality

$$k_6[\text{H}^+][\text{red}] > D/l_{\text{corr}}^2 \quad (4)$$

holds, the probability of  $\text{BrO}_2^*$  turning into  $\text{HBrO}_2$  in the microvolume where a given pair of  $\text{BrO}_2^*$  radicals has been formed is larger than the probability of its escaping from the microvolume. Emerging in the course of reaction R6,  $\text{HBrO}_2$  molecules lower the concentration of bromide in the microvolume further due to reaction R2. Fluctuations are thereby enhanced when the catalyst concentration or activity (i.e., constant  $k_6$ ) grows. When the fluctuation amplitude increases and the rate of system approach to the critical concentration remains unchanged, the time of the critical concentration falling within the range of nonequilibrium fluctuations grows. Therefore, according to our hypothesis, the stirring effect should increase too. The influence of the catalyst concentration on the magnitude of the stirring effect should be strongest when  $k_6[\text{H}^+][\text{red}]$  equals  $D/l_{\text{corr}}^2$ .

To give a more convincing proof of the given statement, it is necessary to make sure that a growth in  $[\text{red}]$  has no effect on the rate of  $[\text{Br}^-]$  approach to the critical concentration. Computer calculations made for schemes R1–R6 with various  $[\text{Ce}^{3+}]_0$  are given in curves 4–7 of Figure 2. From these curves, we notice that the catalyst concentration really has no effect on the rate of  $[\text{Br}^-]$  approach to the critical point.

**Variation in the Type of Catalyst.** According to our hypothesis, primary nonequilibrium fluctuations in bromide concentration arise in the course of diffusion-controlled reaction R1. Then, other nonlinear reactions (for instance R2) enhance these fluctuations. Thus, we can conclude that a replacement of a catalyst should not affect the emergence of fluctuations in

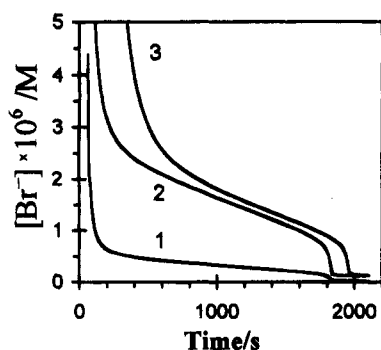


**Figure 3.** Variation of  $[\text{Br}^-]$  vs time in the bromate–bromide–ferroin system calculated on the basis of reactions R1–R5 from Table 1 and reactions R6–R7 from Table 2 at various initial concentrations of bromate and  $\text{H}^+$ . Initial concentrations are  $[\text{ferroin}]_0 = 10^{-4} \text{ M}$  and  $[\text{Br}^-]_0 = 1.73 \times 10^{-4} \text{ M}$ . For curve 1,  $[\text{BrO}_3^-]_0 = 0.01 \text{ M}$ , and  $[\text{H}^+]_0 = 0.8 \text{ M}$ . Curve 2 is obtained by multiplying  $[\text{Br}^-]$  values of curve 1 by a factor of 5, so  $(2) = (1) \times 5$ . For curve 3,  $[\text{BrO}_3^-]_0 = 0.05 \text{ M}$  and  $[\text{H}^+]_0 = 0.16 \text{ M}$ .

the course of reactions R1–R2, but may affect the amplitude of fluctuations and, hence, the magnitude of the stirring effect. However, with the equality of the product  $k_6[\text{H}^+][\text{red}]$  for cerium and ferroin, the effects should be close in magnitude.

**Variation in Bromate Concentration.** On varying  $[\text{BrO}_3^-]$ , we change the critical concentration  $[\text{Br}^-]_{\text{cr}} = k_5[\text{BrO}_3^-]/k_2$  and the exponent  $\gamma$  of  $[\text{HBrO}_2]$  exponential growth, where  $\gamma \approx k_5[\text{H}^+][\text{BrO}_3^-]$ . A decrease in  $[\text{Br}^-]_{\text{cr}}$  should lead to an increase in the relative amplitudes of the Poissonian and, probably, nonequilibrium fluctuations. According to our hypothesis, this should entail the enhancement of the stirring effect with all other conditions and parameters remaining unchanged, i.e., with  $\gamma = \text{constant}$  and  $T_{\text{ind}} = \text{constant}$ . To check our hypothesis, it will be reasonable, therefore, to decrease  $[\text{BrO}_3^-]$  while increasing  $[\text{H}^+]$  so that  $\gamma$  will remain constant.

Computation of the dependence of  $[\text{Br}^-]$  on time with the aforementioned simultaneous variation in  $[\text{BrO}_3^-]_0$  and  $[\text{H}^+]_0$  are shown in Figure 3. It can be seen from a comparison between curves 3 and 2 in Figure 3 that with a 5-fold decrease in  $[\text{BrO}_3^-]_0$  and a simultaneous 5-fold increase in  $[\text{H}^+]_0$ , the time for system approach to the critical concentration remains practically the same while the rate of  $[\text{Br}^-]$  approach to  $[\text{Br}^-]_{\text{cr}}$  measured in absolute units,  $d[\text{Br}^-]/dt$ , decreases by the same factor of 5. By comparison of curves 1 and 3, it is reasonable to suggest that for the system presented by curve 1, the critical concentration,  $[\text{Br}^-]_{\text{cr}}$ , will remain longer in the fluctuation region ( $[\text{Br}^-]$ ,  $[\text{Br}^-] - ((\delta[\text{Br}^-]_{\text{ne}})^2)^{1/2}$ ) because the relative fluctuations  $((\delta[\text{Br}^-]_{\text{ne}})^2)^{1/2}/[\text{Br}^-]$  with smaller  $[\text{Br}^-]$  are enhanced, and the slope of curve 1 is smaller than that of curve 3. Hence, the stirring effect for the conditions of curve 1 should be larger than that for the conditions of curve 3.

**Correlation Length.** According to our hypothesis, the largest effect of the stirring on  $T_{\text{ind}}$  should be at  $L_k \approx l_{\text{corr}}$ . It means that at  $L_k \approx l_{\text{corr}}$ , the slope of the curve  $T_{\text{ind}}(\text{Re})$  will be the steepest. Since  $L_k = d \times \text{Re}^{-3/4}$ , where the Reynolds number  $\text{Re} = ud/\nu_k$ ,  $u$  is the characteristic speed of fluid motion,  $d$  is the characteristic length, and  $\nu_k$  is the kinematic viscosity of water, then for a given  $\text{Re}$  we can uniquely determine  $L_k$ . The situation with  $l_{\text{corr}}$  is much more difficult. An assessment of  $l_{\text{corr}}$  by formula 3 can be done only roughly. More exact estimates might be achieved by deducing correlation functions like  $\langle \delta[B]_i \delta[A]_i \rangle$  and  $\langle \delta[B]_i \delta[B]_j \rangle$  from eqs R1–R6 with additional fluctuation (Langevin) term and diffusion term (like  $\nabla D \nabla$ ) under turbulent stirring, where  $\delta[B]_i$  and  $\delta[A]_i$  are the fluctuations of local concentrations of B and A, respectively. However, this complicated problem has not been solved to date,

and in this work we do not endeavor to give experimental corroboration to the third item of our hypothesis.

### 3. Experimental Section

The reagents  $\text{FeSO}_4 \cdot 7\text{H}_2\text{O}$ , 1,10-phenanthroline, KBr,  $\text{Ce}(\text{NH}_4)_4(\text{SO}_4)_4 \cdot 2\text{H}_2\text{O}$ ,  $\text{H}_2\text{SO}_4$ ,  $\text{NaBrO}_3$ , and malonic acid (MA) were of analytical grade.  $\text{NaBrO}_3$  was additionally purified by double recrystallization from water. Ferroin was prepared by mixing a stock  $\text{Fe}^{\text{II}}$  solution and stock 1,10-phenanthroline solution in a molar ratio of 1:3. To prepare  $\text{Ce}^{\text{III}}$ ,  $\text{Ce}^{\text{IV}}$  was reduced by  $\text{H}_2\text{O}_2$ , and then multiple (3 times) evaporation of the solution and the dissolution of the dry residue in distilled water were followed up to the complete decomposition of  $\text{H}_2\text{O}_2$ . All the solutions were prepared in distilled water.

An autocatalytic  $\text{BrO}_3^-$ – $\text{Br}^-$ –catalyst reaction was run in a batch closed glass cell ( $2 \times 2.2 \times 2.6 \text{ cm}^3$ ), which was thermostatically maintained at  $22 \pm 0.2^\circ \text{C}$ . To avoid contact with the atmosphere (or liquid–gas interphase) and  $\text{Br}_2$  evaporation, the cell was closed with a flat glass cover adhering tightly to its upper edge. To close the cell, the cover was moved horizontally from the side so that a part of the solution from the overfilled cell flew out and no bubble of gas remained in the cell. The efficiency of such a method of isolation was controlled by special experiments that substantiated the unaltered concentration of  $\text{Br}_2$  in the cell for several hours under continuous intensive stirring.

The oscillatory BZ reaction was run in a thermostically controlled cylindrical closed Teflon CSTR (i.d. = 3 cm,  $V_0 = 23 \text{ mL}$ ) with flat quartz windows press-fitted on four sides. The reagents ( $\text{H}_2\text{SO}_4$ ,  $\text{NaBrO}_3$ , ferroin, and MA) were fed in the reactor separately by a peristaltic pump (Model “Zalimp PP2-15”) through the cell bottom, while the reaction mixture flew out through the outlet in the upper stopper which sealed the cell hermetically. The reactor was entirely filled with solution so that no free space and surface were left.

In both cases (batch and flow), stirring was performed with a magnetically driven glass-coated bar (in the case of batch) or magnetically driven Teflon-coated bar (in the case of CSTR) rotating on the bottom of the cell; the glass bar was 2 mm in diameter and 13.5 mm long and the Teflon bar was 8.5 mm in diameter and 12.8 mm long. The rotation rate was varied from 175 to 726 rpm. The stirring intensity was characterized by the Reynolds number  $\text{Re} = ud/\nu_k$ , where  $d$  is the stirrer length from tip to tip,  $u = f_0 \pi d$  ( $f_0$  is the rotation frequency in Hz), and  $\nu_k$  is the kinematic viscosity of water ( $0.01 \text{ cm}^2/\text{s}$ ). A glass stirrer and a glass cell were used to avoid  $\text{Br}_2$  sorption onto their walls. In the case of the oscillatory reaction, the bromine concentration is low because of the high concentration of MA,<sup>40</sup> and  $\text{Br}_2$  sorption on the Teflon reactor walls can be neglected.

The experiments in the batch reactor were conducted as follows. First, the stock solutions of  $\text{H}_2\text{SO}_4$ , KBr, and  $\text{NaBrO}_3$  were mixed in the aforementioned order. Then, with the cell covered, the mixture was stirred for 50 s at maximum intensity. As is shown in Figure 1, at this period the formation of  $\text{Br}_2$  was practically finished (the initial course of kinetic curves is identical with/without a catalyst). After this, we added the aliquot of stock catalyst solution, closed the cell in the aforementioned way, and adjusted the required rotation frequency of the stirrer.

When we used ferroin as a catalyst, the reaction was followed by monitoring [ferriin] by absorbance at 630 nm (absorptivity used for [ferriin] was  $\epsilon_{630} = 620 \text{ M}^{-1} \text{ cm}^{-1}$ ), while in the case of using cerium as a catalyst, the reaction was followed by monitoring  $[\text{Ce}^{\text{IV}}]$  at 401 nm ( $\epsilon_{401} = 800 \text{ M}^{-1} \text{ cm}^{-1}$ ).<sup>36</sup> The

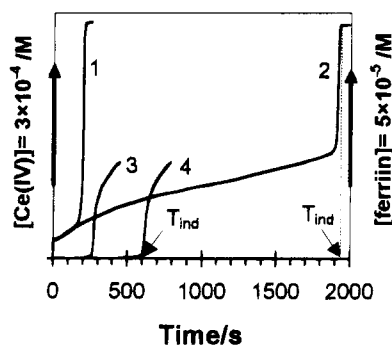


**Figure 4.** Experimental kinetic curves of autocatalytic ferriin (1 and 2) and  $\text{Ce}^{\text{III}}$  (3 and 4) oxidation in the bromate–bromide–catalyst system at various stirring rates. Initial conditions are the following:  $[\text{BrO}_3^-]_0 = 0.01 \text{ M}$ ;  $[\text{H}_2\text{SO}_4]_0 = 0.8 \text{ M}$ . For curves 1 and 2,  $[\text{ferriin}]_0 = 10^{-4} \text{ M}$  and  $[\text{Br}^-]_0 = 1.73 \times 10^{-4} \text{ M}$  with  $\text{Re} = 2190$  for curve 1 and  $\text{Re} = 6920$  for curve 2. For curves 3 and 4,  $[\text{Ce}^{\text{III}}]_0 = 1.28 \times 10^{-3} \text{ M}$  and  $[\text{Br}^-]_0 = 8.65 \times 10^{-5} \text{ M}$  with  $\text{Re} = 2190$  for curve 3 and  $\text{Re} = 6320$  for curve 4.

absorbance of  $[\text{Br}_2]$  at the wavelength  $\lambda = 401 \text{ nm}$  was less than 2% of the  $[\text{Ce}^{\text{IV}}]$  absorbance.

The absorbance was recorded with a homemade spectrophotometric setup. The accuracy of absorption measurement was 0.005 units of optical density  $A$ , which could be measured up to  $A \approx 3$ . The analyzing light from a 100 W iodine-cycle incandescent lamp was incident on the cell after being passed through the first monochromator and a series of lenses. After the cell, the analyzing light passed through the second set of lenses and the second monochromator and was collected on the photocathode of a photoamplifier.

The induction period  $T_{\text{ind}}$  of the autocatalytic reaction was determined as the time from the moment of a catalyst addition up to the moment defined by the intersection point of the time axis and the tangent drawn to the kinetic curve in the place of its maximum slope, as shown in Figure 4.

#### 4. Results and Discussion.

Characteristic kinetic curves of ferriin and  $\text{Ce}^{\text{III}}$  autocatalytic oxidation at various stirring intensities are shown in Figure 4. As is seen from Figure 4, with an increase in Reynolds number, the time  $T_{\text{ind}}$  grows in both cases. We want to emphasize that the effect observed is not in any way related to bromine volatilization. First, bromine volatilization was excluded experimentally owing to special conditions of the experiment. Second, if volatilization had taken place, the stirring effect would have had an opposite sign. In fact, an increase in  $[\text{Br}_2]$  leads to a growth in  $T_{\text{ind}}$ . Hence, if, with the enhancement of the stirring rate, bromine volatilizes more quickly, this should entail a decrease in  $T_{\text{ind}}$ . Indeed, in those special cases, when the experiments on stirring were conducted in the open cell, the induction period and magnitude of the stirring effect decreased in comparison to those in the closed cell.

To test experimentally the first item of our hypothesis, we conducted a series of experiments to determine the dependence of  $T_{\text{ind}}$  on the stirring rate at various  $[\text{Br}^-]_0$ . Figure 5 presents the results of the experiments for the case of ferriin as a catalyst. As is seen from Figure 5, as  $[\text{Br}^-]_0$  increases, the difference between the maximum and minimum  $T_{\text{ind}}$  grows, which fully corresponds to our expectations. To give a quantitative assessment of the effect, we chose the ratio  $T_{\text{ind}}^{\text{max}}/T_{\text{ind}}^{\text{min}}$ , where  $T_{\text{ind}}^{\text{max}}$  and  $T_{\text{ind}}^{\text{min}}$  are the maximum and minimum values of  $T_{\text{ind}}$  at  $\text{Re} = 6930$  and  $\text{Re} = 1700$ , respectively. Figure 6 indicates the experimentally obtained values for  $T_{\text{ind}}^{\text{max}}/T_{\text{ind}}^{\text{min}}$  together with the scaled values of the reciprocal rate of  $[\text{Br}^-]$  approach to the

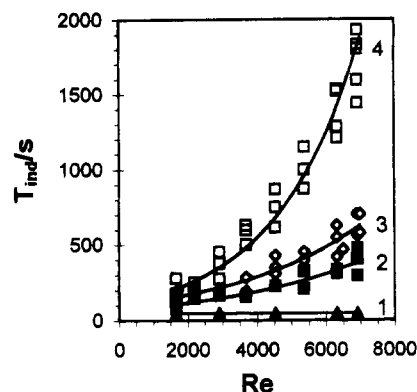


**Figure 5.** Experimental dependencies of the induction period  $T_{\text{ind}}$  on the Reynolds number  $\text{Re}$  for the autocatalytic reaction of ferriin oxidation in the  $\text{BrO}_3^-$ – $\text{Br}^-$ –ferriin system at various  $[\text{Br}^-]_0$ . Initial conditions are the following:  $[\text{BrO}_3^-]_0 = 0.01 \text{ M}$ ;  $[\text{H}_2\text{SO}_4]_0 = 0.8 \text{ M}$ ;  $[\text{ferriin}]_0 = 10^{-4} \text{ M}$ ; (1),  $[\text{Br}^-]_0 = 1.73 \times 10^{-5} \text{ M}$ ; (2),  $[\text{Br}^-]_0 = 4.33 \times 10^{-5} \text{ M}$ ; (3),  $[\text{Br}^-]_0 = 8.65 \times 10^{-5} \text{ M}$ ; (4),  $[\text{Br}^-]_0 = 1.73 \times 10^{-4} \text{ M}$ .

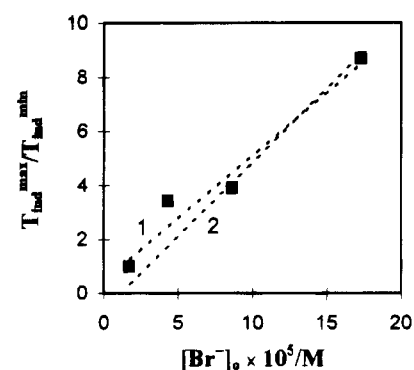


**Figure 6.** Experimental dependence of the magnitude of the stirring effect and calculated dependencies of the reciprocal rate  $(d[\text{Br}^-]/dt)^{-1}$  of  $[\text{Br}^-]$  approach to the critical concentration,  $[\text{Br}^-]_{\text{cr}}$ , on the initial concentration of bromide,  $[\text{Br}^-]_0$ , for the  $\text{BrO}_3^-$ – $\text{Br}^-$ –ferriin reaction. The values  $T_{\text{ind}}^{\text{max}}/T_{\text{ind}}^{\text{min}}$  (■) are obtained from the data presented in Figure 5, while the values  $(d[\text{Br}^-]/dt)^{-1}$  (curves 1 and 2) are obtained from the calculated kinetic curves similar to those shown in Figure 2. Curves 1 and 2 are the result of simulation of reactions R1–R6 and R1–R7, respectively.

critical concentration  $[\text{Br}^-]_{\text{cr}}$ ,  $(d[\text{Br}^-]/dt)^{-1}$ , at various  $[\text{Br}^-]_0$  and with ferriin as a catalyst. The values of  $(d[\text{Br}^-]/dt)^{-1}$  were obtained from the calculated curves of  $[\text{Br}^-]$  vs time (see Figure 2) with regard to reaction R7 (curve 1 in Figure 6) and without it (curve 2 in Figure 6). A numerical coefficient  $k_s$  of scaling, by which the values of  $(d[\text{Br}^-]/dt)^{-1}$  were multiplied, was selected so that the resulting curves passed near the experimental points  $T_{\text{ind}}^{\text{max}}/T_{\text{ind}}^{\text{min}}$ . For curve 1  $k_s = 0.52 \times 10^{-8} \text{ M/s}$ , and for curve 2  $k_s = 0.18 \times 10^{-8} \text{ M/s}$ . The value  $(d[\text{Br}^-]/dt)^{-1}$  is proportional to the time of the system residing near the critical point. Satisfactory coincidence of the theoretical and experimental curves in Figure 6 may substantiate our hypothesis.

To test the second item of our hypothesis, we determined the dependence of  $T_{\text{ind}}$  on  $\text{Re}$  at various concentrations of a catalyst. Some results of the experiments with cerium as a catalyst are shown in Figure 7. No stirring effect was observed at low  $[\text{Ce}^{\text{III}}]_0$  ( $[\text{Ce}^{\text{III}}]_0 < 2 \times 10^{-4} \text{ M}$ ) comparable to the concentration of ferriin in the aforementioned experiments. The effect appeared only at a considerable increase in  $[\text{Ce}^{\text{III}}]_0$ , when  $[\text{Ce}^{\text{III}}]_0 = 10^{-3}$ – $10^{-2} \text{ M}$ . It is noteworthy that the rate of  $[\text{Br}^-]$  approach to the critical concentration, according to the reaction scheme R1–R6, is independent of  $[\text{Ce}^{\text{III}}]_0$  at  $[\text{Ce}^{\text{III}}]_0 > 10^{-4} \text{ M}$  (see Figure 2) while the exponent  $\gamma$  of the exponential  $[\text{Ce}^{\text{IV}}]$  growth for  $[\text{Ce}^{\text{III}}]_0 = 6.41 \times 10^{-3} \text{ M}$  (curve 2 in Figure 7) is 2 times larger than that for  $[\text{Ce}^{\text{III}}]_0 = 3.42 \times 10^{-4} \text{ M}$  (curve 1 in

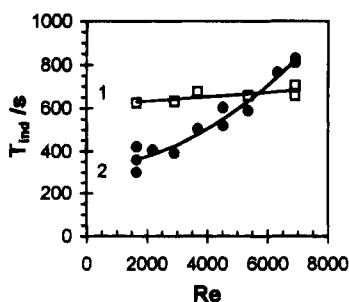


**Figure 7.** Dependence of the induction period  $T_{\text{ind}}$  on the Reynolds number  $Re$  for the autocatalytic  $\text{Ce}^{\text{III}}$  oxidation in the  $\text{BrO}_3^-$ – $\text{Br}^-$ – $\text{Ce}^{\text{III}}$  system at various  $[\text{Ce}^{\text{III}}]_0$ . Initial conditions are the following:  $[\text{BrO}_3^-]_0 = 0.01 \text{ M}$ ;  $[\text{H}_2\text{SO}_4]_0 = 0.85 \text{ M}$ ;  $[\text{Br}^-]_0 = 1.73 \times 10^{-4} \text{ M}$ ; (1),  $[\text{Ce}^{\text{III}}]_0 = 3.42 \times 10^{-4} \text{ M}$ ; (2),  $[\text{Ce}^{\text{III}}]_0 = 6.41 \times 10^{-3} \text{ M}$ .

**TABLE 3:**  $T_{\text{ind}}^{\text{max}}$  and  $T_{\text{ind}}^{\text{min}}$  Induction Periods of Autocatalytic  $\text{BrO}_3^-$ – $\text{Br}^-$ –Cerium Reaction at Stirring Rotation Rates of 726 ( $Re = 6970$ ) and 175 rpm ( $Re = 1700$ ), Respectively, and Their Ratio  $T_{\text{ind}}^{\text{max}}/T_{\text{ind}}^{\text{min}}$  at Various Initial Concentrations  $[\text{Ce}^{\text{III}}]_0^a$

$[\text{Ce}^{\text{III}}]_0/\text{M}$	$T_{\text{ind}}^{\text{max}}/\text{s}$	$T_{\text{ind}}^{\text{min}}/\text{s}$	$T_{\text{ind}}^{\text{max}}/T_{\text{ind}}^{\text{min}}$
$10^{-4}$	600	570	1.05
$1.28 \times 10^{-3}$	500	265	1.88
$6.41 \times 10^{-3}$	400	130	3.0
$3.42 \times 10^{-4}$	650	600	1.08
$6.41 \times 10^{-3}$	825	375	2.2

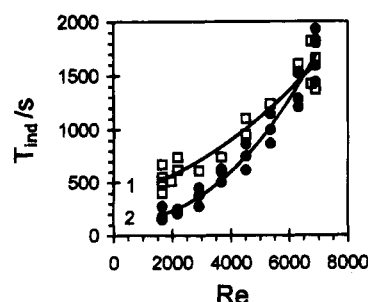
<sup>a</sup> Conditions:  $[\text{H}_2\text{SO}_4]_0 = 0.8 \text{ M}$ ;  $[\text{BrO}_3^-]_0 = 0.01 \text{ M}$ ;  $[\text{Br}^-]_0 = 8.65 \times 10^{-5} \text{ M}$  for rows 1–3;  $[\text{H}_2\text{SO}_4]_0 = 0.85 \text{ M}$ ;  $[\text{BrO}_3^-]_0 = 0.01 \text{ M}$ ;  $[\text{Br}^-]_0 = 1.73 \times 10^{-4} \text{ M}$  for the last two rows.

Figure 7). A growth in  $\gamma$  should entail a larger fluctuation amplitude. The dependence of the magnitude ( $T_{\text{ind}}^{\text{max}}/T_{\text{ind}}^{\text{min}}$ ) of the stirring effect on  $[\text{Ce}^{\text{III}}]_0$  with various initial concentrations of bromide is shown in Table 3. As is seen from Table 3, when the  $[\text{Ce}^{\text{III}}]_0$  grows, the effect is enhanced, which also corroborates our hypothesis.

It is of interest to compare the magnitudes of the stirring effect in cerium and ferriox systems at the analogous initial concentrations of  $\text{H}_2\text{SO}_4$ ,  $\text{BrO}_3^-$ , and  $\text{Br}^-$ . For the ferriox system, at  $[\text{H}_2\text{SO}_4]_0 = 0.8 \text{ M}$ ,  $[\text{BrO}_3^-]_0 = 0.01 \text{ M}$ , and  $[\text{ferriox}]_0 = 10^{-4} \text{ M}$ , the value  $T_{\text{ind}}^{\text{max}}/T_{\text{ind}}^{\text{min}}$  equals about 3–4 in the case of  $[\text{Br}^-]_0 = 8.65 \times 10^{-5} \text{ M}$  and about 8–9 in the case of  $[\text{Br}^-]_0 = 1.73 \times 10^{-4} \text{ M}$ . For the cerium system, with the same values of  $[\text{H}_2\text{SO}_4]_0$ ,  $[\text{BrO}_3^-]_0$ , and  $[\text{Br}^-]_0 = (0.86\text{--}1.8) \times 10^{-4} \text{ M}$ , the value  $T_{\text{ind}}^{\text{max}}/T_{\text{ind}}^{\text{min}}$  equals 2–3 at  $[\text{Ce}^{\text{III}}]_0 = 6.4 \times 10^{-3} \text{ M}$ . The product  $k_6[\text{red}]$  in the case of cerium equals  $8 \times 10^4 \times 6.4 \times 10^{-3} = 512 \text{ M}^{-1} \text{ s}^{-1}$ , while with ferriox it equals  $(10^7\text{--}10^8) \times 10^{-4} = 10^3\text{--}10^4 \text{ M}^{-1} \text{ s}^{-1}$ . Hence, it follows that the larger the  $k_6[\text{red}]$ , the larger the  $T_{\text{ind}}^{\text{max}}/T_{\text{ind}}^{\text{min}}$ . It means that of most importance for the stirring effect is the rate of the  $\text{BrO}_2^*$  radical turning into  $\text{HBrO}_2$ , i.e., the product  $k_6[\text{red}]$ , not the reaction rate constant of a catalyst interaction with the  $\text{BrO}_2^*$  radical (constant  $k_6$ ). Recall that the growth of the aforementioned rate leads to an increase in the amplitude of nonequilibrium fluctuations resulting, according to our hypothesis, from fast nonlinear reactions R1 and R2. These conclusions also substantiate our hypothesis.

The results of the experiments on the effect of  $[\text{BrO}_3^-]_0$  on  $T_{\text{ind}}$  and on the magnitude of the stirring effect are shown in Figure 8 and in Table 4. As is seen from Figure 8 and Table 4, the stirring effect is enhanced with a  $[\text{BrO}_3^-]_0$  decrease, both with  $\gamma = \text{constant}$  (compare curves 1 and 2 in Figure 8 and rows 1 and 2 in Table 4) and without it (compare rows 1–3 and rows 4 and 5 in Table 4). This fact also substantiates our hypothesis.

Thus, all theoretical predictions considered in part 2 gained experimental evidence. It only remains to be shown that the



**Figure 8.** Dependence of the induction period  $T_{\text{ind}}$  on the Reynolds number  $Re$  for the autocatalytic reaction of ferriox oxidation in the  $\text{BrO}_3^-$ – $\text{Br}^-$ –ferriox system at various initial concentrations of bromate. Initial conditions are the following:  $[\text{Br}^-]_0 = 1.73 \times 10^{-4} \text{ M}$ ;  $[\text{ferriox}]_0 = 10^{-4} \text{ M}$ ; (1),  $[\text{BrO}_3^-]_0 = 0.05 \text{ M}$  and  $[\text{H}_2\text{SO}_4]_0 = 0.16 \text{ M}$ ; (2),  $[\text{BrO}_3^-]_0 = 0.01 \text{ M}$  and  $[\text{H}_2\text{SO}_4]_0 = 0.8 \text{ M}$ .

**TABLE 4:**  $T_{\text{ind}}^{\text{max}}$  and  $T_{\text{ind}}^{\text{min}}$  Induction Periods of the Autocatalytic  $\text{BrO}_3^-$ – $\text{Br}^-$ –Ferriox Reaction at Stirring Rotation Rates of 726 ( $Re = 6970$ ) and 175 rpm ( $Re = 1700$ ), Respectively, and Their Ratio  $T_{\text{ind}}^{\text{max}}/T_{\text{ind}}^{\text{min}}$  at Various Initial Concentrations  $[\text{BrO}_3^-]_0$  and  $[\text{H}_2\text{SO}_4]_0^a$

$[\text{BrO}_3^-]_0/\text{M}$	$[\text{H}_2\text{SO}_4]_0/\text{M}$	$T_{\text{ind}}^{\text{max}}/\text{s}$	$T_{\text{ind}}^{\text{min}}/\text{s}$	$T_{\text{ind}}^{\text{max}}/T_{\text{ind}}^{\text{min}}$
0.05	0.16	1590	530	3
0.01	0.8	1800	190	9.5
0.0025	1.5	>8000	450	>17
0.0025	1.5	3000	340	8.8
0.01	0.8	50	50	1.0

<sup>a</sup> Conditions:  $[\text{ferriox}]_0 = 10^{-4} \text{ M}$ ;  $[\text{Br}^-]_0 = 1.73 \times 10^{-4} \text{ M}$  for rows 1–3;  $[\text{Br}^-]_0 = 1.73 \times 10^{-5} \text{ M}$  for rows 4 and 5.

**TABLE 5:** Oscillation Periods  $T_{\text{max}}$  and  $T_{\text{min}}$  of the BZ Reaction under CSTR at Stirring Rates of 571 and 342 rpm, Respectively, and Their Ratio  $T_{\text{max}}/T_{\text{min}}$  at Various Initial Concentrations  $[\text{BrO}_3^-]_0^a$

$[\text{BrO}_3^-]_0/\text{M}$	$T_{\text{max}}/\text{s}$	$T_{\text{min}}/\text{s}$	$T_{\text{max}}/T_{\text{min}}$
0.1	17.5	17.15	1.02
0.02	150	102	1.47
0.01	620	275	2.25
0.1 <sup>b</sup>	183	165	1.11

<sup>a</sup> Conditions:  $[\text{H}_2\text{SO}_4]_0 = 0.8 \text{ M}$ ;  $[\text{ferriox}]_0 = 0.87 \text{ mM}$ ;  $[\text{MA}]_0 = 0.25 \text{ M}$ ,  $\tau_0 = 60 \text{ min}$ ;  $V_0 = 23 \text{ mL}$ . <sup>b</sup>  $[\text{H}_2\text{SO}_4]_0 = 0.2 \text{ M}$  and  $[\text{ferriox}]_0 = 2.8 \text{ mM}$ .

stirring effect in the oscillatory BZ reaction and the variation of the induction period in the autocatalytic  $\text{BrO}_3^-$ – $\text{Br}^-$ –catalyst reaction can be explained analogously. To illustrate this statement we studied the effect of stirring on the oscillation period at various initial concentrations of bromate. The results of variation in  $T_{\text{max}}/T_{\text{min}}$ , where  $T_{\text{max}}$  is the oscillation period at 571 rpm and  $T_{\text{min}}$  is the oscillation period at 342 rpm, are presented in Table 5. The oscillation run at  $[\text{BrO}_3^-]_0 = 0.01 \text{ M}$  is presented in Supporting Information. As is seen from Table 5, with a decrease in  $[\text{BrO}_3^-]_0$  the stirring effect grows, which is in full accord with the dependence of the stirring effect on  $[\text{BrO}_3^-]_0$  for the induction period. The last row of Table 5 shows the magnitude of the stirring effect at  $[\text{BrO}_3^-]_0 = 0.1 \text{ M}$  and  $[\text{H}_2\text{SO}_4]_0 = 0.2 \text{ M}$ . As was the case with the autocatalytic reaction where we tried to keep  $\gamma = \text{constant}$  and  $T_{\text{ind}} = \text{constant}$  at various  $[\text{BrO}_3^-]_0$ , we lowered  $[\text{H}_2\text{SO}_4]_0$  at  $[\text{BrO}_3^-]_0 = 0.1 \text{ M}$  until the oscillation period became nearly equal to the oscillation period for the case of  $[\text{H}_2\text{SO}_4]_0 = 0.8 \text{ M}$  and  $[\text{BrO}_3^-]_0 = 0.02 \text{ M}$ . As is evident from the comparison between the results obtained for these two sets of concentrations, the effect is larger in the case of the smaller concentration of bromate ( $T_{\text{max}}/T_{\text{min}} = 1.11$  and  $1.47$ ). The results from Table 5 correspond to the reaction run in CSTR with a residence time  $\tau_0 = 60 \text{ min}$ . The analogous results were also obtained under



batch conditions. Thus, probable inhomogeneities in the mixing of the feedstreams play no part in our case of CSTR. All this stresses once more that of most importance for the stirring effect are the duration of a system's stay near the critical point  $[\text{Br}^-]_{\text{cr}}$  and the relative fluctuation amplitude, which should grow with a decrease in  $[\text{BrO}_3^-]_0$  and, consequently,  $[\text{Br}^-]_{\text{cr}}$ .

**Nature of Fluctuations.** The experimental material stated above testifies to the validity of the hypothesis suggested and, consequently, to the fact that the stirring effect is accounted for by the influence of the intensity of turbulent mass mixing on the amplitude and lifetime of nonequilibrium concentration fluctuations. P. Ruoff suggested<sup>4</sup> that such fluctuations result from the interaction between the local thermal and concentration fluctuations.

We adhere to some other point of view. We suppose that nonequilibrium concentration fluctuations resulting from the random character of chemical reactions in MVs may affect macrokinetics under isothermal conditions as well. These fluctuations may develop by the following mechanism. At first, as a result of fast reactions R1–R2, nonequilibrium fluctuations of  $[\text{Br}^-]$  and  $[\text{HBrO}_2]$ , symmetrical about the averages, spontaneously arise (cluster-formation effect<sup>29</sup>). Let us refer to the microvolumes with  $[\text{Br}^-]_i < [\text{Br}^-]$  and  $[\text{HBrO}_2]_i > [\text{HBrO}_2]$  as positive fluctuations and microvolumes with  $[\text{Br}^-]_i > [\text{Br}^-]$  and  $[\text{HBrO}_2]_i < [\text{HBrO}_2]$  as negative fluctuations; subscript "i" denotes the local concentration. Due to the autocatalytic instability (reactions R5 + 2(R6)) and to the reaction between activator ( $\text{HBrO}_2$ ) and inhibitor ( $\text{Br}^-$ ), positive and negative fluctuations have a different amplification factor. This can be easily illustrated by the calculated curve of  $[\text{HBrO}_2]$  growth (curve 4 in Figure 1). The slope of the tangent to the curve,  $\gamma_i$ , equals the exponent of  $[\text{HBrO}_2]$  growth at a given moment of time  $t$ . The higher the  $[\text{HBrO}_2]$ , the larger the  $\gamma_i$ . The maximum slope of the tangent,  $\gamma$ , equals approximately  $k_5[\text{BrO}_3^-][\text{H}^+]$ , which is in accord with the experimentally obtained exponential growth factor for the oxidized form of a catalyst. For the positive and negative fluctuations with the corresponding values of  $[\text{HBrO}_2]_+$  and  $[\text{HBrO}_2]_-$  such that  $[\text{HBrO}_2]_+ > [\text{HBrO}_2]_-$ , and with corresponding values of  $\gamma_+$  and  $\gamma_-$ , an inequality 5 results:

$$\gamma_- < \gamma_+ \quad (5)$$

Denote the time at which a given MV can be considered to be isolated from the rest of the volume as  $\tau_n$ . Then, at a time  $\tau_n$ ,  $[\text{HBrO}_2]$  will increase in positive and negative fluctuations by about a factor of  $\exp(\gamma_+\tau_n)$  and  $\exp(\gamma_-\tau_n)$ , respectively. Due to inequality 5, for the amplification factors  $\exp(\gamma_+\tau_n)$  and  $\exp(\gamma_-\tau_n)$ , inequality 6 results:

$$e^{\gamma_+\tau_n} < e^{\gamma_-\tau_n} \quad (6)$$

Such a varying amplification of fluctuation brings about a situation where, after a time  $\tau_n$ , in MVs with positive fluctuations  $[\text{HBrO}_2]_+$  will grow, and  $[\text{Br}^-]_+$  will decrease to a much larger extent than in MVs with negative fluctuations. This allows us to coin an unusual term "asymmetrical" fluctuations to specify the difference in amplification of positive and negative "symmetrical" fluctuations.

After a time  $\tau_n$ , "asymmetrical" fluctuations mix with the whole bulk and change the average concentration, these changes being more pronounced than those in the analogous "nonfluctuating" system. This fact is reflected in the inequality of the following type:

$$e^{\gamma_+\tau_n} + e^{\gamma_-\tau_n} > 2e^{\gamma_i\tau_n} \quad (7)$$

where the exponent  $\gamma_i$  for a "nonfluctuating" system lies in the range  $(\gamma_+, \gamma_-)$  and equals about  $(\gamma_+ + \gamma_-)/2$ . Inequality 7 is true for  $\gamma_i \leq (\gamma_+ + \gamma_-)/2$  or for  $\tau_n > \ln 2/(\gamma_+ - \gamma_-)$ . The magnitude (or measure) of asymmetry of nonequilibrium fluctuations determines the magnitude of their effect on the dynamics of the averages. Fluctuation asymmetry may be expected to reach its maximum when the slope of the tangent to curve 4 in Figure 1 varies to the greatest degree at a small variation in  $[\text{HBrO}_2]$ , as well as when the times  $\tau_n$  are long such that  $\gamma\tau_n \geq 1$ . The maximum of fluctuations  $\delta\gamma_i$  is achieved at the maximum of the second derivative to curve 4 (Figure 1) in close proximity to the critical point,  $[\text{Br}^-]_{\text{cr}}$  (see Supporting Information). This fact indicates that it is in the critical point and that in its immediate vicinity the effect of fluctuations on the dynamics of the averages is the largest.

A qualitative explanation given here is based on the asymmetry of fluctuations rather than on the presence of nuclei in the system. Although the presence of nuclei should undoubtedly assist the stirring effect near the critical point, we can mention here at least one fact which makes us doubt their decisive role in the stirring effect. Times  $T_{\text{ind}}^{\text{max}}$  and  $T_{\text{ind}}^{\text{min}}$  for the experimental conditions plotted in curve 4 of Figure 5 equal approximately 1800 and 180 s, respectively. As is seen from the calculated curve 1 (Figure 3) simulating the same conditions, for the times 100–200 s the bromide concentration is 3–10 times larger than  $[\text{Br}^-]_{\text{cr}}$ , while with small Re, the  $[\text{Br}^-]$  fluctuations should notably affect the averages and  $T_{\text{ind}}$  even at  $[\text{Br}^-] \cong (5-10)[\text{Br}^-]_{\text{cr}} \cong 10^{-6}$  M. For the values  $l_{\text{corr}} \cong 20 \mu\text{m}$  and  $[\text{Br}^-] \cong 10^{-6}$  M, the magnitude of Poissonian fluctuations is  $(10^{-4}-10^{-3})[\text{Br}^-]$ . Hence, for the nuclei to occur, i.e., for the inequality  $[\text{Br}^-]_i < [\text{Br}^-]_{\text{cr}}$  to hold, nonequilibrium fluctuations should be  $10^4-10^5$  times as large as the Poissonian ones. Probably, this is possible, but to date we do not know any mechanism for that large amplification of the fluctuation amplitude. In the case of asymmetrical fluctuations, an amplification factor for the Poissonian fluctuations may be considerably smaller than  $10^4$  and reach several units or tens. According to our assumptions this factor depends on two nonlinear processes: the effect of cluster-formation due to reaction R1 and partly to R2 and the autocatalysis in the presence of inhibitor,  $\text{Br}^-$ , i.e., on reactions R5–R6 and R2.

There is one more problem related to both the existence of nuclei and asymmetrical fluctuations. It consists of the fact that the lifetime  $\tau_n$  of spatial fluctuations, being smaller or comparable to the Kolmogorov length,  $L_k$ , is much shorter than the characteristic time of an autocatalytic reaction  $\gamma^{-1}$ . In fact, the time  $\tau_n$  relates to the Reynolds number as  $t_{\text{mix}}\text{Re}^{-1/2}$  and ranges between 1 and 100 ms,<sup>21a</sup> where  $t_{\text{mix}}$  is the experimentally found time of dye droplet mixing, while  $\gamma^{-1}$  ranges between 1 and 10 s, and  $\gamma\tau_n < 1$ . Consequently, this raises the question of whether the fluctuations in short-living MVs are amplified to the extent ( $< \exp(\gamma\tau_n)$ ) large enough to make them responsible for the stirring effect. Ruoff managed to simulate<sup>4</sup> the stirring effect in the BZ reaction only on condition that the lifetime of the nuclei was about 1 s. It is probable that at small Reynolds number ( $\text{Re} < 2000$ ), there exist in a reactor some poorly stirred and long-lived regions, such as a cone in the reactor center or by-wall layers. Even for a well-developed turbulence, the long-lived coherent structures consisting of vortex tubes were predicted theoretically on the basis of the lattice model.<sup>42</sup>

Thus, for the development of asymmetrical large-scale fluctuations at small Re of most importance should be two values:  $\tau_n$  and  $\delta\gamma_i$ , where  $\delta\gamma_i$  is the fluctuation amplitude of  $[\text{HBrO}_2]$  exponential growth at a moment  $t$ . The larger the value of  $\delta\gamma_i$ , the closer the system is to the critical concentration.

Some authors hold to another hypothesis for stirring effects in closed reactors.<sup>11,18</sup> Under this hypothesis stirring affects the rate constants of the diffusion-controlled reactions: the reactions between radicals of malonic acid,  $\text{MA}^\bullet$ , and  $\text{BrO}_2^\bullet$ , and the reactions of disproportionation of radicals  $\text{MA}^\bullet$ ,  $\text{BrO}_2^\bullet$ , and  $\text{Br}^\bullet$ . It follows from the present work that the stirring effect occurs in the system even without organic substrate, and, hence, it cannot be connected with the reactions of  $\text{MA}^\bullet$  radicals. It is worth mentioning, however, that the known effect of cluster-formation peculiar to diffusion-controlled reactions without stirring<sup>29</sup> slows down these reactions and causes something like a decrease in the effective rate constant, whereas stirring should slightly magnify this constant. Thus, the emergence of micro-heterogeneous clusters may, in fact, lead to a slight decrease in the observed rate constant,  $k_d$ , of a diffusion-controlled reaction. According to our calculation, a 10% decrease of constant  $k_1$  (reaction R1) entails a 5–10% growth of the induction period  $T_{\text{ind}}$ , while a 10-fold decrease of  $k_1$  makes  $T_{\text{ind}}$  4 times longer. In the experiment, however, we observe a 10-fold decrease of the induction period with a smaller stirring rate. That is, the effect has an opposite sign and, hence, cannot be accounted for by the effect of stirring on the rate constant of a diffusion-controlled reaction.

## 5. Conclusion

Using an autocatalytic  $\text{BrO}_3^- - \text{Br}^-$  – catalyst reaction and closed classical BZ reaction as an example, we supported experimentally the hypothesis suggested in which the stirring effect is determined by the rate of system approach to the critical point and by the amplitude of nonequilibrium asymmetrical fluctuations. The lower the rate and the larger the fluctuation amplitude, the larger the stirring effect. We also showed that by varying the initial concentrations of reagents, we could efficiently control these values and the stirring effect.

**Acknowledgment.** The research described in this publication was made possible in part by Grant MQCOOO from the International Science Foundation and was supported in part by the Russian Foundation for Fundamental Investigations through Research Grant 93-03-4090.

**Supporting Information Available:** Chemical system that corresponds to eqs 1 and 2 and its detailed description with Figure 1S, kinetic curves of  $[\text{Br}^-]$  vs time in the bromate–bromide–ferroin system (Figure 2S), kinetic run of the oscillatory ferroin-catalyzed BZ reaction at different stirring conditions (Figure 3S), and kinetic curve of  $\log[\text{HBrO}_2]$  vs time and its second derivative in the bromate–bromide– $\text{Ce}^{\text{III}}$  system (Figure 4S) (8 pages). Ordering information is available on any current masthead page.

## References and Notes

- (1) Puhl, A.; Altares, V.; Nicolis, G. *Phys. Rev. A* **1988**, *37*, 3039.
- (2) (a) Boissonade, J.; DeKepper, P. *J. Chem. Phys.* **1987**, *87*, 210. (b) De Kepper, P.; Boissonade, J. In *Fluctuations and Sensitivity in Nonequilibrium Systems*; Horsthemke, W., Kondepudi, D. K., Eds.; Springer: Berlin, 1984.
- (3) Horsthemke, W.; Hannon, L. *J. Chem. Phys.* **1984**, *81*, 4363.
- (4) Ruoff, P. *J. Phys. Chem.* **1993**, *97*, 6405.

- (5) Deering, W. D.; West, B. J. *J. Stat. Physics* **1991**, *65*, 1247.
- (6) Mazo, R. M.; Guslander, J. *J. Phys. Chem.* **1992**, *96*, 3958.
- (7) (a) Epstein, I. R. *Nature* **1990**, *346*, 16. (b) Epstein, I. R. *Nature* **1995**, *374*, 321.
- (8) Sagues, F.; Sancho, J. M. *J. Chem. Phys.* **1988**, *89*, 3793.
- (9) Dewel, G.; Borckmans, P.; Walgraef, D. *Phys. Rev. A* **1985**, *31*, 1983.
- (10) Aronovitz, J. A.; Nelson, D. R. *Phys. Rev. A* **1984**, *29*, 2012.
- (11) (a) Hlaváčová, J.; Sevcík, P. *J. Phys. Chem.* **1994**, *98*, 6304. (b) Hlaváčová, J.; Sevcík, P. *Chem. Phys. Lett.* **1993**, *201*, 242.
- (12) Gyorgyi, L.; Field, R. J. *J. Phys. Chem.* **1992**, *96*, 1220.
- (13) Ganapathisubramanian, N. *J. Phys. Chem.* **1991**, *95*, 3005.
- (14) Roux, J. C.; DeKepper, P.; Boissonade, J. *Phys. Lett. A* **1983**, *97*, 168.
- (15) (a) Ruoff, P. *Chem. Phys. Lett.* **1982**, *90*, 76. (b) Ruoff, P.; Schwitters, B. *Z. Phys. Chem. (Wiesbaden)* **1983**, *135*, 171.
- (16) (a) Menzinger, M.; Jankowski, P. *J. Phys. Chem.* **1990**, *94*, 4123. (b) Ali, F.; Menzinger, M. *J. Phys. Chem.* **1992**, *96*, 1511. (c) Menzinger, M.; Jankowski, P. *J. Phys. Chem.* **1986**, *90*, 1217. (d) Dutt, A. K.; Menzinger, M. *J. Phys. Chem.* **1990**, *94*, 4867.
- (17) Patonay, G.; Noszticzius, Z. *React. Kinet. Catal. Lett.* **1981**, *17* (1–2), 187.
- (18) Noszticzius, Z.; Bodnar, Z.; Garamszegi, L.; Wittmann, M. *J. Phys. Chem.* **1991**, *95*, 6575.
- (19) Li, R.-S.; Li, J. *Chem. Phys. Lett.* **1988**, *144*, 96.
- (20) (a) Nagypal, I.; Epstein, I. R. *J. Chem. Phys.* **1988**, *89*, 6925. (b) Nagypal, I.; Epstein, I. R. *J. Phys. Chem.* **1986**, *90*, 6285.
- (21) (a) Vanag, V. K.; Alfimov, M. V. *J. Phys. Chem.* **1993**, *97*, 1884. (b) Vanag, V. K.; Ait, A. O. *Russ. J. Phys. Chem.* **1993**, *67*, 2024. (c) Melikhov, D. P.; Vanag, V. K.; *Russ. J. Phys. Chem.* **1994**, *68*, 1019. (d) Melikhov, D. P.; Vanag, V. K.; *Russ. J. Phys. Chem.* in press.
- (22) Lopez-Tomas, L.; Sagues, F. *J. Phys. Chem.* **1991**, *95*, 701.
- (23) Pojman, J. A.; Dedeaux, H.; Fortenberry, D. *J. Phys. Chem.* **1992**, *96*, 7331.
- (24) Kumpinsky, E.; Epstein, I. R. *J. Chem. Phys.* **1985**, *82*, 53.
- (25) (a) Sevcík, P.; Adamčíková, I. *Chem. Phys. Lett.* **1988**, *146*, 419. (b) Sevcík, P.; Adamčíková, I. *J. Chem. Phys.* **1989**, *91*, 1012.
- (26) Hauser, M. J. B.; Lebender, D.; Schneider, F. W. *J. Phys. Chem.* **1992**, *96*, 9332.
- (27) Nicolis, G.; Prigogine, I. *Self-Organization in Nonequilibrium Systems*; New-York: Wiley, 1977.
- (28) Boissonade, J. *Physica A* **1982**, *113*, 607.
- (29) (a) Ovchinnikov, A. A.; Zeldovich, Ya. B. *Chem. Phys.* **1978**, *28*, 215. (b) Burlatsky, S. F.; Ovchinnikov, A. A. *Sov. Phys. JETP* **1986**, *43*, 494. (c) Toussaint, D.; Wilczek, F. *J. Chem. Phys.* **1983**, *78*, 2642. (d) Sokolov, I. M.; Argyrakis, P.; Blumen, A. *J. Phys. Chem.* **1994**, *98*, 7256.
- (30) Gardiner, C. W.; McNeil, K. J.; Walls, D. F.; Matheson, I. S. *J. Stat. Phys.* **1976**, *14*, 307.
- (31) (a) Kondepudi, D. K. Theory of Noise Induced Processes in Special Applications. In *Noise in Nonlinear Dynamical Systems*; Moss, F., McClintock, P. V. E., Eds.; Cambridge University Press: New York, 1989; Vol. 2, Chapter 10. (b) Kondepudi, D. K.; Gao, M. *J. Phys. Rev. A* **1987**, *35*, 340.
- (32) Zeldovich, Ya. B.; Mikhailov, A. S. *Usp. Fiz. Nauk* **1987**, *153* (3), 469.
- (33) Keizer, J. *Statistical Thermodynamics of Nonequilibrium Processes*; New York: Springer-Verlag, 1987.
- (34) Landau, L. D.; Lifschitz, E. M. *Fluid Mechanics*; Oxford: Pergamon, 1959.
- (35) Noyes, R. M.; Field, R. J.; Thompson, R. C. *J. Am. Chem. Soc.* **1971**, *93*, 7315.
- (36) Field, R. J.; Försterling, H.-D. *J. Phys. Chem.* **1986**, *90*, 5400.
- (37) Geer, C. W. *Numerical Initial Value Problems in Ordinary Differential Equations*; Prentice-Hall, Inc.: NJ, 1971.
- (38) Kéki, S.; Magyar, I.; Beck, M. T.; Gáspár, V. *J. Phys. Chem.* **1992**, *96*, 1725.
- (39) (a) Sasaki, Y. *Bull. Chem. Soc. Jpn* **1990**, *63*, 3521. (b) Ige, J.; Ojo, F.; Olubuyide, O. *Can. J. Chem.* **1979**, *57*, 2065.
- (40) Franck, U. F.; Geiseler, W. *Naturwissenschaften* **1971**, *58*, 52.
- (41) Schilt, A. A. *Analytical Application of 1,10-Phenanthroline and Related Compounds*; Pergamon: Oxford 1969.
- (42) Taguchi, Y.-h.; Takayasu, H. *Physica D* **1993**, *69*, 366.
- (43) Zhabotinsky, A. M.; Buchholtz, F.; Kiyatkin, A. B.; Epstein, J. *Phys. Chem.* **1993**, *97*, 7578.

JP951521P